Cerebral Cortex December 2014;24:3209–3220
doi:10.1093/cercor/bht181
Advance Access publication July 12, 2013

Body-Centered, Mixed, but not Hand-Centered Coding of Visual Targets in the Medial Posterior Parietal Cortex During Reaches in 3D Space

K. Hadjidimitrakis[1,2], F. Bertozzi[1,2], R. Breveglieri[1,2], P. Fattori[1,2] and C. Galletti[1,2]

[1]Department of Human and General Physiology and [2]Department of Pharmacy and Biotechnology, University of Bologna, Bologna 40126, Italy

Address correspondence to Prof. Patrizia Fattori, Department of Pharmacy and Biotechnology, University of Bologna, Piazza di Porta San Donato 2, Bologna 40126, Italy. E-mail: patrizia.fattori@unibo.it
Kostas Hadjidimitrakis and Federica Bertozzi contributed equally to this work.
Kostas Hadjidimitrakis and Patrizia Fattori are equal corresponding authors.

The frames of reference used by neurons in posterior parietal cortex (PPC) to encode spatial locations during arm reaching movements is a debated topic in modern neurophysiology. Traditionally, target location, encoded in retinocentric reference frame (RF) in caudal PPC, was assumed to be serially transformed to body-centered and then hand-centered coordinates rostrally. However, recent studies suggest that these transformations occur within a single area. The caudal PPC area V6A has been shown to represent reach targets in eye-centered, body-centered, and a combination of both RFs, but the presence of hand-centered coding has not been yet investigated. To examine this issue, 141 single neurons were recorded from V6A in 2 *Macaca fascicularis* monkeys while they performed a foveated reaching task in darkness. The targets were presented at different distances and lateralities from the body and were reached from initial hand positions located at different depths. Most V6A cells used body-centered, or mixed body- and hand-centered coordinates. Only a few neurons used pure hand-centered coordinates, thus clearly distinguishing V6A from nearby PPC regions. Our findings support the view of a gradual RF transformation in PPC and also highlight the impact of mixed frames of reference.

Keywords: arm position, depth, reach, reference frame, visuomotor transformation

Introduction

The PPC is implicated in the reference frame (RF) transformations that underlie visually guided reaching movements. The information about target location is encoded first in a retinotopic frame of reference (eye-centered) and then into a coordinate system referred to the body and the hand (Flanders et al. 1992). It was initially suggested that this transformation takes place serially in PPC, that is, caudal PPC areas encode reach targets in eye-centered RF, whereas the rostral ones use hand-centered coordinates (Lacquaniti et al. 1995; Batista et al. 1999; Buneo et al. 2002, 2008; Marzocchi et al. 2008). However, recent studies have revealed that both RFs exist in most PPC regions, with many neurons encoding mixed eye- and hand-centered target representations (Chang et al. 2009; Chang and Snyder 2010; McGuire and Sabes 2011; Buneo and Andersen 2012). As a result, there is still a debate on which RFs are used in PPC areas and on the importance of intermediate representations in the visuomotor transformations that take place in PPC (McGuire and Sabes 2011; Bremner and Andersen 2012).

In most previous studies, target and eye/hand positions were varied in a bidimensional frontal plane. Only 2 studies, to our knowledge, investigated in PPC the encoding of reaching targets in depths (Bhattacharyya et al. 2009; Ferraina et al. 2009). Bhattacharyya et al. (2009) studied the integration of disparity and vergence signals in the parietal reach region (PRR) during preparation of reach movements toward targets placed at different distances along midsagittal plane. They found that PRR neurons encoded target depth in eye-centered coordinates, but the influence of hand signals was not tested. This was examined by Ferraina et al. (2009) in area 5. They found that most area 5 neurons encoded targets relative to the hand and only a few encoded targets relative to the eye.

In both the above reported studies, targets were placed in a restricted part of the workspace, as they were varied in depth but not in direction. In the present study, we addressed the above questions, by using targets distributed at various depths and directions within the animal's workspace, while the neural activity was recorded from the medial PPC area V6A, where many neurons are spatially tuned during reaches (Fattori et al. 2001, 2005). A previous study reported that an important fraction of V6A neurons do encode targets in eye-centered coordinates (Marzocchi et al. 2008), though the majority used an intermediate eye- and body-centered representation. Here, we specifically tested whether hand-centered coding of reach targets occurs in V6A. We found that most neurons encoded target location either relative to the body or in mixed body- and hand-centered coordinates, but the evidence for hand-centered representations was very weak. Our findings confirm that V6A is involved in the early stages of visuomotor transformations for reaching, supporting the view of a caudo-rostral trend, from eye- to hand-centered representation, in the PPC of the superior parietal lobule. Furthermore, it is evident in V6A, like in many other PPC areas, neurons mostly represent reaching targets in mixed frames of reference, with the eye/body representation prevailing caudally, and the body/hand one rostrally.

Materials and Methods

General Procedures

Two male macaque monkeys (*Macaca fascicularis*) weighing 4.4 and 6 kg were used. Initially, the animals were habituated to sit in a primate chair and interact with the experimenters. Then, a head-restraint system and a recording chamber were surgically implanted under general anesthesia (sodium thiopenthal, 8 mg/kg*h, i.v.) following the procedures reported by Galletti et al. (1995). A full program of postoperative analgesia (ketorolac tromethamine, 1 mg/kg i.m. immediately after surgery, and 1.6 mg/kg i.m. on the following days)

and antibiotic care (Ritardomicina, benzatinic benzylpenicillin + dihydrostreptomycin + streptomycin, 1–1.4 ml/10 kg every 5–6 days) followed surgery. Experiments were performed in accordance with national laws on care and use of laboratory animals and with the European Communities Council Directive of 24 November, 1986 (86/609/EEC) and that of 22 September 2010 (2010/63/EU). All the experimental protocols were approved by the Bioethical Committee of the University of Bologna. During training and recording sessions, particular care was taken to avoid any behavioral and clinical sign of pain or distress.

Extracellular recording techniques and procedures to reconstruct microelectrode penetrations were similar to those described in other reports (e.g., Galletti et al. 1996). Single cell activity was extracellularly recorded from the anterior bank of the parieto-occipital sulcus. Area V6A was initially recognized on functional grounds following the criteria described in Galletti et al. (1999), and later confirmed following the cytoarchitectonic criteria according to Luppino et al. (2005). We performed multiple electrode penetrations using a 5-channel multielectrode recording system (Thomas Recording). The electrode signals were amplified (at a gain of 10 000) and filtered (bandpass between 0.5 and 5 kHz). Action potentials in each channel were isolated with a waveform discriminator (Multi Spike Detector; Alpha Omega Engineering) and were sampled at 100 kHz.

Recording Locations

Histological reconstructions have been performed following the procedures detailed in a recent publication from our lab (Gamberini et al. 2011). Briefly, electrode tracks and the approximate location of each recording site were reconstructed on histological sections of the brain on the basis of electrolytic lesions and several other cues, such as the coordinates of penetrations within recording chamber, the kind of cortical areas passed through before reaching the region of interest, the depths of passage points between gray and white matter. All neurons of the present work were assigned to area V6A.

Behavioral Paradigm

Electrophysiological signals were collected while monkeys were performing a reaching task in darkness using the hand contralateral to the recording hemisphere. During the task, the monkeys maintained steady fixation of the reaching targets with their head restrained. The task was performed in 2 blocks that differed in the starting position of the hand: in both cases, the starting position was on the midsagittal plane at waist level. In one block, the hand started from a button, near button, placed 4 cm in front of monkey's chest, on the mid-sagittal line, (Fig. 1*A*) and in the other, it started from a button, far button, located 14 cm farther from the near one (Fig. 1*B*). In each block only one of the 2 buttons was available to press, whereas the other was covered. For each neuron, the block sequence was random. Although technical limitations did not allow a complete randomization of the trials of the 2 initial hand positions, several controls were performed to remove potential artifacts of signal instability (see below). Fixation and reaching targets were 9 Light Emitting Diodes (LEDs) positioned at eye level, at three different distances and directions (Fig. 1*A*,*B*). Three LEDs targets were placed at three isovergence angles: the nearest targets were located at 10 cm from the eyes (17.1°) and the LEDs located at intermediate and far positions were at a depth of 15 cm (11.4°) and 25 cm (6.9°), respectively. At each isovergence angle, LEDs were positioned in three directions: one central, along the sagittal midline and 2 lateral, at iso-version angles of −15° and +15°. Targets positions were selected in order to be within the peripersonal space.

The time sequence of the task is shown in Figure 1*C*. A trial began when the monkey pressed the button (HB press). After 1000 ms, 1 of the 9 LEDs lit up green (LEDon) and this cue instructed the monkey to fixate it, while maintaining the button pressed. Then, the monkey had to wait 1000–2000 ms for a change in color of the fixation LED (green to red) without performing any eye or arm movement. The color change was the go-signal (GO) for the animal to release the button and start an arm movement (M) toward the foveated target. Then, the monkey held its hand on the target for 800–1200 ms (H), keeping the gaze fixed on the same LED. The switching off of the target (Redoff) cued the monkey to release the target and return to the button (HB press) in order to receive reward. The presentation of stimuli and the animal's performance were monitored using custom software written in Labview (National Instruments), as described previously (Kutz et al. 2005). Eye position signals were sampled with 2 cameras (1 for each eye) of an infrared oculometer system (ISCAN) at 100 Hz and were controlled by an electronic window (4 × 4°) centred on the fixation target. If the monkey fixated outside this window, the trial was aborted. The task was performed in darkness, in blocks of 90 randomized trials, 10 for each LED target. The background light was switched on briefly between blocks to avoid dark adaptation.

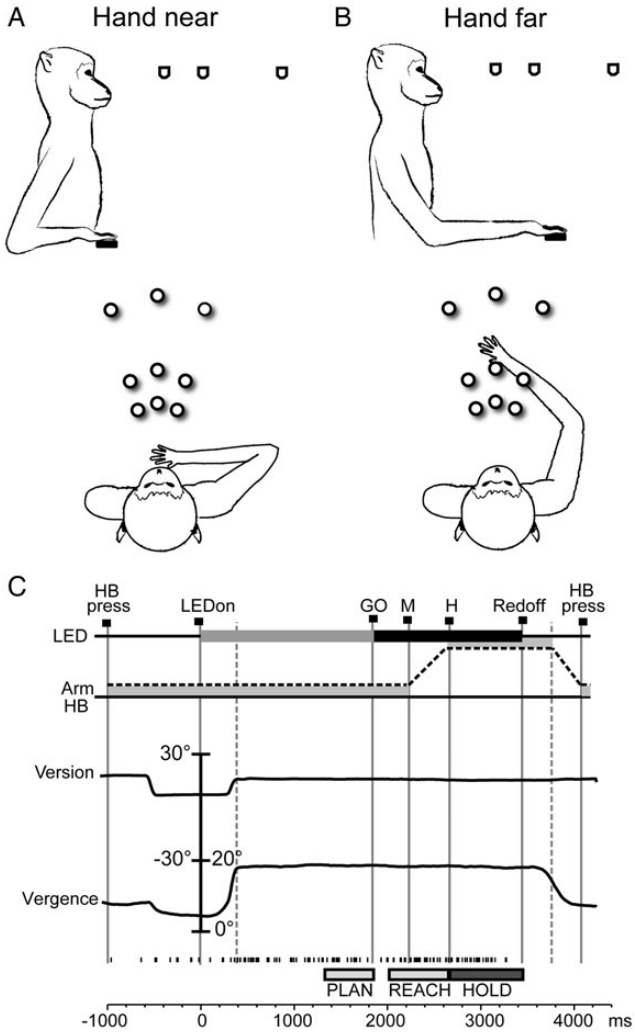

Figure 1. Experimental setup and task sequence. (*A*, *B*) Side (upper panels) and top (lower panels) view of the reaching in depth setup task. Eye and hand movements were performed in darkness toward 1 of the 9 LEDs located at eye level at different depths and directions from one initial hand position located next to the body (*A*) and from another being 14 cm farther (*B*). (*C*) Time sequence of task events with LED and arm status, the eye's vergence and version traces and the spike train of neural activity during a single trial. From left to right vertical continuous lines indicate: trial start (HB press), target appearance (LEDon), go signal (GO), start of the arm movement period (M), beginning of the holding the target period (H), switching off of the LED (Redoff), and trial end (HB press). Long vertical dashed line indicates the end of the saccade (left) and the start of the returning arm movement (right).

At the start of each recording session, monkeys were required to perform a calibration task where they fixated 10 LEDs mounted on a frontal panel at a distance of 15 cm from the eyes. For each eye, signals to be used for calibration were extracted during fixation of 5 LEDs, 1 central aligned with the eye's straight ahead position and 4 peripheral placed at an angle of ±15° (distance: 4 cm) both in the horizontal and vertical axes. From the 2 individual calibrated eye position signals, we derived the mean of the 2 eyes (the conjugate or

version signal), and the difference between the 2 eyes (the disconjugate or vergence signal) using the equations: version = (R + L)/2 and vergence = R−L, where R and L was the position of the right and left eye, respectively.

Data Analysis

Neural activity was studied in 2 epochs: the PLAN epoch that corresponded to the last 500 ms before the GO signal, and the REACH epoch that started 200 ms before the arm movement onset (M) and ended at the pressing of the LED target (Fig. 1*C*). To check the stability of the recorded units between the 2 blocks, we used the HOLD epoch, as a reference. This epoch started with the pressing of the LED target (H) and ended with the switching off of the target (Redoff). For a given LED, the activity in that period was assumed to be equal in the 2 blocks since the visual, eye position and arm somatosensory signals were identical. To test this, we performed a *t*-test ($P < 0.001$) for each cell, comparing the 9 mean firing rates (1 mean per LED) of the HOLD epoch recorded in the 2 blocks. Neurons having a significantly different activity in the HOLD epoch between the 2 blocks were excluded. A very similar procedure has been employed in other studies of reaching activity (e.g., Chang et al. 2008). Using this control, 40 of 181 cells (22%) of the initial population were not studied further. In addition, the visual inspection of the raster histograms and the distribution of the interspike intervals were used as additional controls, and they were in good agreement with the comparison of the HOLD activity. Of the remaining, stable cells (141), 86 were recorded from the first and 55 from the second monkey. For further analysis, only cells tested in at least 7 trials per position and also had a mean firing rate higher than 5 spikes/s for at least 1 target position were selected. The reasons for this conservative choice are linked to the implicit high variability of biological responses and are explained in detail in Kutz et al. (2003). Significant modulation of neural activity relative to different positions of the reach targets or to different initial hand positions was studied with a 2-way analysis of variance (ANOVA) performed for the PLAN and the REACH epochs (factor 1: target position, factor 2: initial hand position). The neural modulation relative to ANOVA's factors was assessed when factor 1 and/or factor 2 and/or the interaction factor 1 × 2 were significant ($P < 0.05$).

Population Analysis of Reference Frames

Given that the target was foveated and the head of the animals was fixed, our experiment cannot distinguish body from head- and eye-centered frames of reference. To study whether neurons encode the target in body- or in hand-centered coordinates we compared the mean firing rates of single conditions: 1) where targets that had the same location relative to the body were reached from different hand positions (Fig. 3*A*, left), and 2) where targets having the same location with respect to the hand were reached (Fig. 3*B*, left). At the population level, the similarity of the paired firing rates was evaluated calculating the Pearson correlation coefficient (Zar 1999). A Z-test ($P < 0.05$) was used to compare the correlation coefficients.

Euclidean Distance Analysis of Reference Frames

At single cell level, to compare the similarity of firing rates in body- and in hand-centered RFs we calculated in each cell the average activity of all the conditions that were equivalent in each frame. The means in each pair were compared after constructing their 95% confidence interval (CI) using bootstrap (500 iterations). Cells could have significantly different firing rates between condition pairs in both RFs. To find which RF accounted more for the neural responses, we quantified the similarity between the mean firing rates in each frame by computing the normalized Euclidean distance between them (Batista et al. 2007).

$$\sqrt{\frac{\sum_{i=1}^{T}(n_i - m_i)^2}{T}} \qquad (1)$$

The mean PLAN/REACH activity for targets n and m that were equivalent in a given RF were normalized between 0 and 1 and T corresponds to the targets number. The 95% CIs on the distance value were estimated using a bootstrap test ($n = 500$). Neurons falling outside of one of these intervals are sensitive to one RF, whereas neurons falling inside these 2 CIs are influenced by both RFs. For each neuron, a synthetic mean firing rate was computed by averaging the activity of randomly resampled trials. For each configuration, this was done twice and the distance between these synthetic firing rates was calculated using equation (1). This procedure was repeated 500 times and the average value was computed. Then the distance values for each pair of configurations were averaged. Using this computation, we obtained 2 values for each neuron, which were plotted against one another; they represented the noise values. Using these estimates of measurement for the population, we determined a border that encompassed 95% of the noise values (Fig. 4*A*). Neurons plotted under this border had sensitivity not statistically distinguishable from zero. To compare the RFs of single cells in PLAN and REACH, we used their Euclidean distance values in each frame to calculate a single RF index. To compute the RF index, individual data points from Figure 4*A,B* were projected on the negative diagonal line. The RF index was equal to the distance of the projection point from the upper end of the negative diagonal line that had Euclidean coordinates 0 and 1. As a result the RF index ranged from 0 to 1.414. Small index values (<0.5) indicate stronger effect of body-centered coordinates, whereas RF index values equal to 1 or higher indicate a prevalence of hand-centered coding.

Separability Analysis

We applied the singular value decomposition (SVD) analysis (Pena and Konishi 2001; Pesaran et al. 2006; Bhattacharyya et al. 2009; Blohm et al. 2009; Blohm 2012) to examine whether in single neurons target location was separable from starting hand position. A 2D matrix M was constructed from the mean activity across target and hand conditions. This matrix was subsequently reconstructed to calculate the diagonal matrix S than contained the singular values. The fractional energy (FE) of the first singular value was computed from the equation below:

$$\mathrm{FE} = \frac{s_i}{\sum_i s_i^2}$$

Neural responses were classified as separable if the first singular value was significantly larger ($P < 0.05$) compared with the first singular value calculated when conditions were randomized by permuting (Randomization test, 1000 permutations) the rows and the columns of the initial 2D matrix (Pesaran et al. 2006; Bhattacharyya et al. 2009).

Modulation Indexes

To measure the relative strength of the modulations by target location in body- and hand centered coordinates, we calculated 2 indexes in the same way to that used in area PRR to quantify the modulations of reaching activity by disparity and vergence angle (Bhattacharyya et al. 2009). Index T_B, referring to target in body coordinates, quantified the modulation between pairs of conditions where the target position with respect to the body changed while the movement vector was constant.

$$\mathrm{Index}\,T_B = \frac{(\max - \min)}{(\max + \min)}$$

As already shown in Figure 3*B*, left, our experimental configuration permitted us to have three pairs of equal movement vectors for each neuron. The three indexes T_B were subsequently averaged for each neuron to obtain a single index.

Index T_H, referring to target in hand-centered coordinates, measured the strength of the gain modulation by hand position while target position remained the same.

$$\mathrm{Index}\,T_H = \frac{(\max - \min)}{(\max + \min)}$$

Index T_H was obtained by averaging the 9 indexes calculated from the 9 pairs of conditions with the same reaching target and different initial

hand positions. To compare the 2 indexes, we subtracted Index T_H from Index T_B for each neuron to determine if the firing rate was more influenced by changing the body-centered target location (T_B) or the movement vector (T_H).

Vector Correlation

Each 2D matrix was transformed to a 2D vector field that described the gradient of the response (calculated using the Matlab gradient function). To calculate the estimate of vector correlation, we used the method first developed by Hanson et al. (1992) to analyze geographic data. By applying this method, a correlation coefficient ρ that is analogous to the Pearson correlation coefficient was calculated. This coefficient quantified how much the 2D vector fields are related to each other. Apart from the coefficient, the method defines the amount of rotation or reflection and the scaling between the 2 vector fields. If x and y are the 2 dimensions of 1 vector field, and u and v the dimensions of the other, using the following equation from Hanson et al. (1992) a correlation coefficient ρ is calculated:

$$\rho = \sqrt{\frac{(\sigma_{xu}^2 + \sigma_{yv}^2 + \sigma_{xv}^2 + \sigma_{yu}^2 + 2s\xi)}{(\sigma_x^2 + \sigma_y^2)(\sigma_u^2 + \sigma_v^2)}}$$

where

$$\xi = \sigma_{xu} * \sigma_{yv} - \sigma_{xv} * \sigma_{yu}$$
$$s = sgn(\xi) = \frac{\xi}{\xi}$$

and σ_x^2, σ_y^2, σ_u^2, and σ_v^2 are the variances of x, y, u, v and σ_{xu}, σ_{yv},σ_{xv}, and σ_{yu} are the covariances of the 4 dimensions. A scale factor (β) and a phase angle (θ) can also be calculated:

$$\beta = s * \rho\sqrt{\frac{\sigma_u^2 + \sigma_v^2}{\sigma_x^2 + \sigma_y^2}}$$
$$\theta = atan\left(\frac{\sigma_{xv} - s\sigma_{yu}}{\sigma_{xu} - s\sigma_{yv}}\right)$$

The coefficient ρ has a range from −1 to 1, with 1 characterizing a perfect rotational relationship between the 2 vector fields and −1 denoting that one vector field can be produced by the reflection of the other along a given axis. The phase angle θ has a range from −180° to 180° and quantifies the angle of rotation or reflection that is necessary to align the 2 vector fields, whereas the factor β represents the gain relationship between the fields. All methods of analysis gave consistent results between the 2 monkeys, and are therefore presented together. All analyses were performed using custom scripts written in MATLAB (Mathworks, Natick, MA, USA).

Results

We analyzed the firing rate of 141 stable, well-isolated neurons recorded in V6A in 2 *Macaca fascicularis* during the planning (PLAN) and execution (REACH) of arm reaching movements. Task configuration and data analyses were designed in order to study the frames of reference, and in particular to probe the existence of hand-centered representation of reach goals. To this end, each target was reached from 2 different hand positions, one next to the trunk (Fig. 1*A*) and the other 14 cm in front of it (Fig. 1*B*). Thus, target position relative to the body remained constant while the position changed relative to the hand. Reaches were directed to LED targets arranged at various directions and depths within the animals' peripersonal space (Fig. 1*A,B*). A 2-way ANOVA was performed to find cells with planning and reaching activity significantly ($P < 0.05$) influenced by target position and initial hand position (Table 1). A well-represented group of tuned cells were affected only by target location (PLAN: 45%, REACH: 36%); a second group showed a main effect of both target and initial hand position (PLAN: 23%, REACH: 29%). Very few cells were modulated by the initial hand position only (4% in both epochs). Neurons with interaction between the 2 factors (multiplicative effect) were 13% and 27% in PLAN and in REACH epoch, respectively.

Table 1
Incidence of the effect of target and initial hand position in each epoch

Epoch	Target position only (%)	Initial hand position (%)	Both (%)	Interaction (%)
PLAN	45.3	4.3	23.1	12.8
REACH	35.7	4	28.6	27

Figure 2 shows examples of typical neuronal modulations. The neuron in Figure 2*A* discharged maximally during reaches toward far LEDs. Reach-related activity significantly decreased for intermediate targets and ceased completely for near targets. This strong spatial tuning occurred in both PLAN and REACH epochs and was very similar for different initial hand positions. It should be noted that the nearest targets required outward reaches when the hand started from near button, but inward reaches when the hand started from far button: in spite of this, neuronal activity was nearly the same. In summary, this neuron encoded the spatial location of target relative to the body regardless of the initial hand position. Figure 2*B* illustrates an example of the other most frequent neural behavior, that is, neurons modulated by both initial hand position and target position. In contrast with the neuron in Figure 2*A*, this cell was activated only in REACH epoch. When the hand started from the near button, the REACH activity was highest for reaches toward targets located at intermediate and near distances. Changing the starting position of the hand from near to far button evoked an increase of REACH activity for all targets without altering the spatial tuning. The neuron in Figure 2*C* showed an interaction effect between target and initial hand position. When monkey performed reaches with the hand starting next to the body, there was an augmenting of REACH activity with increasing movement amplitude, resulting in preference for the far targets. In contrast, when reaches started far from the body, the spatial tuning of REACH activity almost disappeared. The PLAN activity of this cell was low, but consistently tuned in the 2 blocks of reaches, and showed a gain effect of initial hand position.

Population Analyses of Reference Frames

To reach a target, the brain may calculate the difference between target and hand position, that is, the movement vector. Spatial arrangement of initial hand positions and of targets in our experimental setup resulted in a variety of movement vectors. For example, to reach the nearest and the intermediate targets from the far button monkeys performed inward movements (Fig. 1*B*), whereas in all other cases, they executed outward movements. Apart from comparison between the neural effects of inward and outward movements, our experimental configuration allowed us to compare the effect on neuronal activity of reach movements of different amplitude and direction toward the same spatial location (Fig. 3*A*), and the effect of movements of the same amplitude and direction toward different spatial locations (Fig. 3*B*).

To define the RF in which targets were encoded, we plotted the activity of each modulated cell in pairs of conditions: 1)

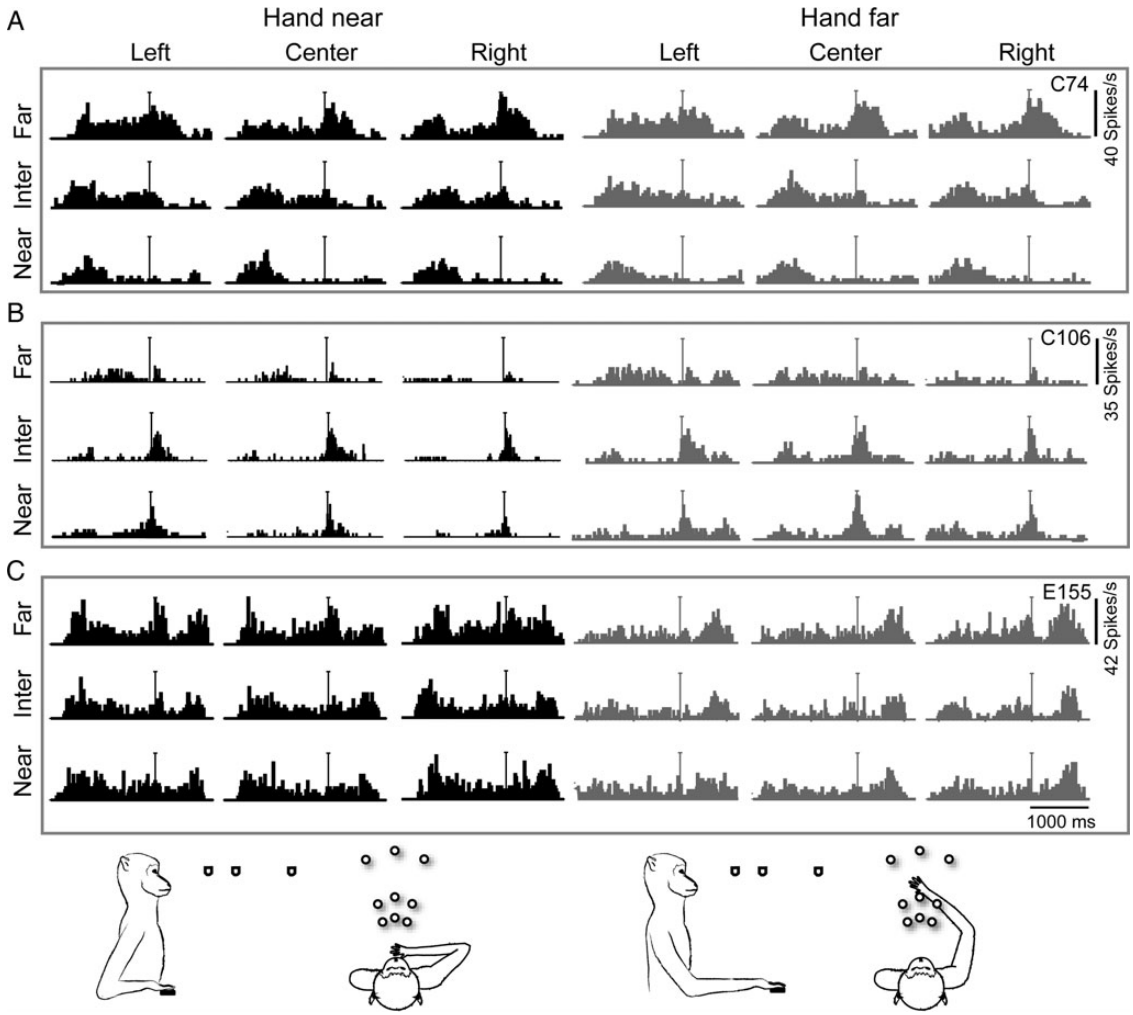

Figure 2. Example neurons with target and initial hand position tuning in both PLAN and REACH epochs. (*A–C*) Spike histograms for the 9 target positions, arranged at 3 directions (columns) and 3 depths (rows). (*A*) Neuron showing similar tuning for different initial hand positions. (*B*) Neuron modulated by both target location and initial hand position. (*C*) Neuron showing an interaction between target position and initial hand position. Vertical lines indicate the alignment of activity at the start of arm movement. REACH epoch starts 200 ms before this time point.

where the target was constant in body-centered coordinates but differed in hand-centered coordinates (Fig. 3*A*, left), and 2) where the movement vector was constant but the target location with respect to the body was different (Fig. 3*B*, left). The scatter plots in Figure 3*A*,*B* illustrate at population level how similar were the firing rates within each frame of reference in PLAN (Fig. 3*A*,*B*, middle panels) and REACH (Fig. 3*A*, *B*, right panels) epochs. In Figure 3*A*, we paired the mean firing rates for reaching with different movement vectors, but constant target location with respect to the body. Each neuron was plotted 9 times because there were 9 pairs of such conditions. In Figure 3*B*, we paired the mean reach-related activity of conditions where targets were located in the same position with respect to the hand (same movement vector), but in different positions in space. Each cell was plotted 3 times since there were 3 pairs of conditions with the same movement vector, that is near and far LEDs reached from the near and far button, respectively, in each direction (Fig. 3*B*, left). A low scatter (high correlation) indicates that a particular RF accounts well for the population activity. Figure 3*A*,*B* show that both RFs gave a good fit of neural activity. However, the correlation was significantly stronger (*Z*-test, $P < 0.05$) when the target remained in the same position with respect to the body, that is, in body-centered frame of reference ($r = 0.83$ in PLAN and $r = 0.88$ in REACH) than when the movement vector remained constant, that is, in hand-centered frame of reference ($r = 0.67$ in PLAN and $r = 0.66$ in REACH). It could be argued that these high r values were due to the correlations between positions with low firing rates (<10 sp/s). To account for this, we calculated the r values taking into account only the pairs were at least one of the 2 conditions had activity equal or higher than 10 spikes per second. Excluding the pairs with low firing rates decreased the r values by 11–25%, but the correlations were still strong and highly significant. Similar strong correlation was found when the near targets were reached from near and far initial hand position (Fig. 3*C*). In this case, movements of constant amplitude, but of opposite direction (i.e., inward vs. outward movements) were executed. Again, this confirmed the strong influence of body-centered target location.

To directly compare in single cells the effect of changing target location in the 2 RFs, we calculated the Euclidean distance metric, which is a measure of cell sensitivity to each RF (Batista et al. 2007). For each neuron and epoch, we computed the Euclidean distance twice by comparing the pairs of

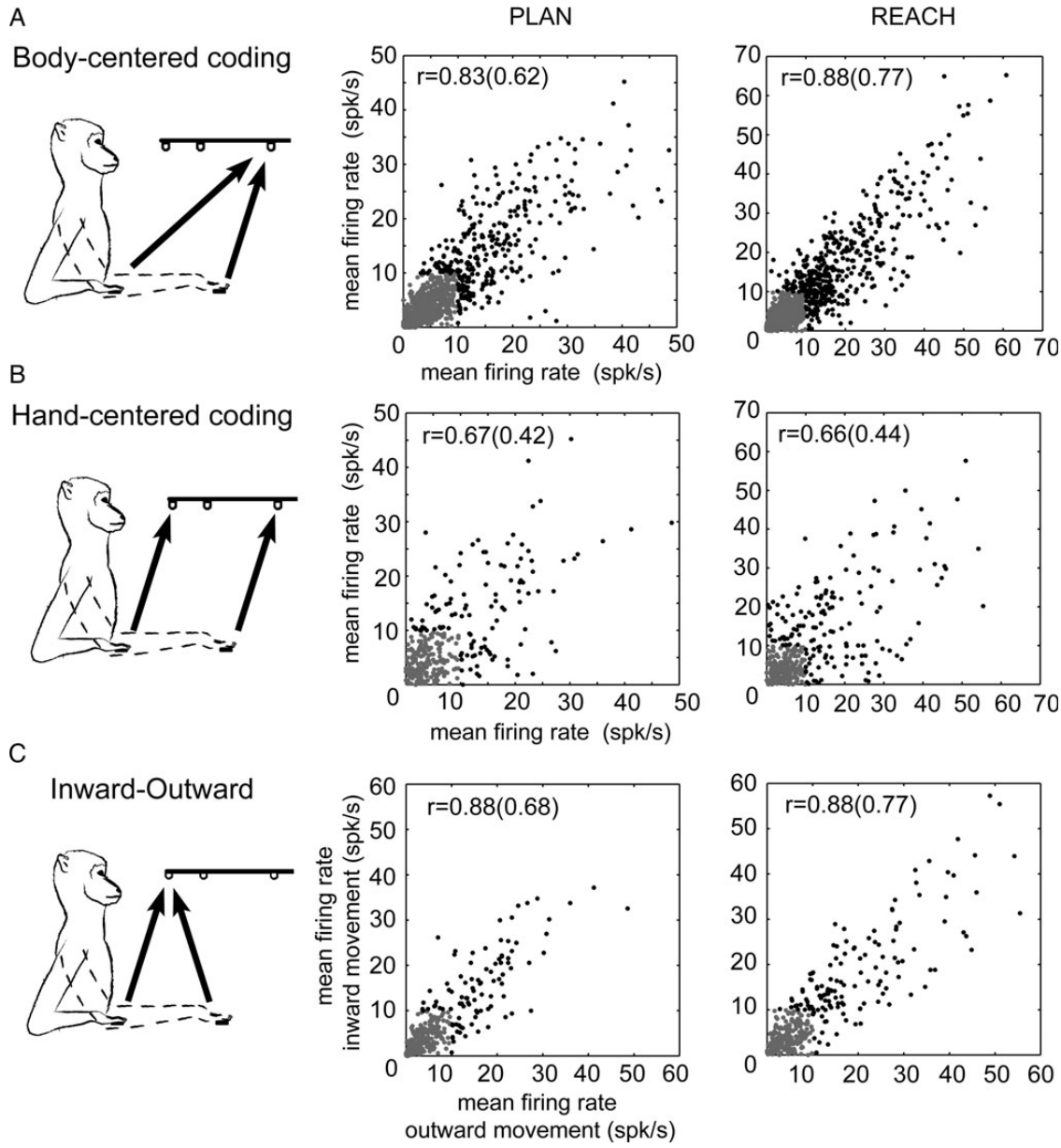

Figure 3. Correlation analysis of the reference frames of PLAN and REACH activity for the population of V6A modulated cells. (*A*) Left: Pairs of movements for targets having the same position in body coordinates. Middle/Right: Scatter plots of the neural activity in PLAN/REACH of pairs of movements toward targets that were identical in body-centered coordinates. (*B*) Left: Pairs of movements for targets having the same position in hand coordinates. Middle/Right: Scatter plots of the neural activity in PLAN/REACH of pairs of movements to targets that were identical in hand-centered frame of reference. (*C*) Left: Scheme of hand and target configuration for pairs of movements toward targets having the same location with respect to the body and associated with a movement vector of equal amplitude and opposite direction. Middle/Right: Scatter plots of the corresponding activity during PLAN and REACH, respectively. The correlation is significantly higher ($P < 0.05$) when body coordinates are kept constant. In all scatter plots, correlation coefficient values were computed twice, either including all pairs (black and gray points, *r* values outside parentheses), or taking into account only the pairs where at least one of the conditions had activity ≥10 sp/s (black points, *r* values inside parentheses).

conditions that were equivalent in each RF (see Materials and Methods section). Figure 4*A* illustrates a plot of the 2 distances calculated in each cell in the PLAN (top panel) and REACH (bottom panel) epochs. A neuron encoding reach targets in a hand-centered RF is expected to have a large Euclidean distance value along the abscissa and a small value along the ordinate, whereas a neuron using a body-centered frame would show the opposite behavior. We also calculated the confidence intervals of the Euclidean distances. Neurons with confidence intervals that did not cross the equality line are illustrated with filled circles in Figure 4*A*, whereas those with intervals crossing the equality line with empty circles. Using this analysis we divided V6A neurons into 3 categories (see Fig. 4*A*): 1) neurons that encoded reach goal in body-centered coordinates (filled circles above the equality line; about 29% and 38% in PLAN and REACH epoch, respectively), 2) neurons encoding target positions in hand-centered coordinates (filled circles below the equality line; about 2% in both PLAN and REACH epochs), and 3) neurons that were equally sensitive to both the body-centered and the hand-centered locations of the targets (empty circles; about 40% in PLAN and 41% in REACH epochs). The prevalence of body-centered encoding became even more evident when

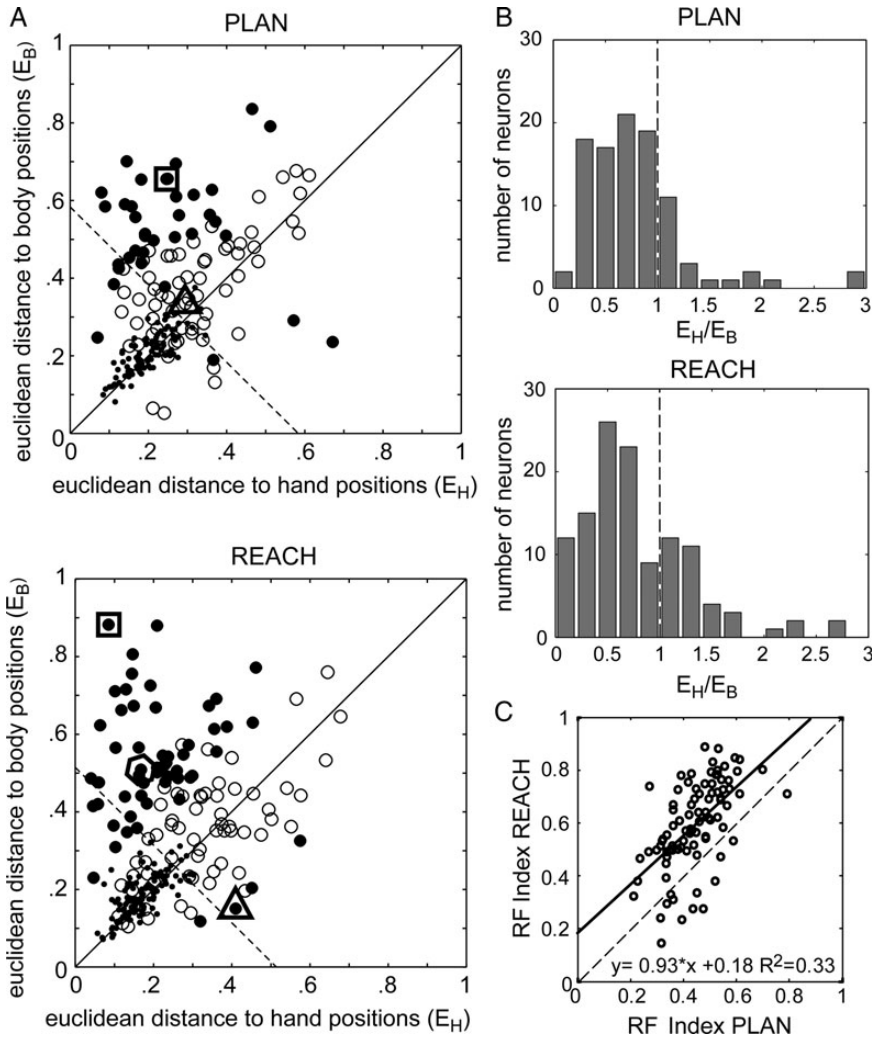

Figure 4. Population analysis of the reference frames of PLAN and REACH activity. (*A*) Each data point represents one neuron, showing its sensitivity, calculated as Euclidean distance, in a body-centered and in a hand-centered frame in PLAN (top) and REACH (bottom) epochs. Filled circles represent neurons with significantly (bootstrap estimated, $n = 500$, $P < 0.05$) different sensitivities. Empty circles represent neurons with equal sensitivities. The dashed line indicates the level below which differences could be due to noise. V6A population has very few hand-centered neurons and an equal amount of body-centered and mixed hand/body-centered neurons. The circles inside the square, hexagon, and triangle indicate the example neurons of Figure 2*A,B*, and *C*, respectively (see also Fig. 7). (*B*) Population histograms of the ratio of hand versus body euclidean distances (E_H/E_B) for PLAN (top) and REACH (bottom) epochs. The distribution was unimodal with most cells having a larger E_B than E_H. The vertical dashed line highlights that most ratios were <1. (*C*) Reference frame consistency across epochs. Scatter plot of the reference frame (RF) index in PLAN versus REACH of the neurons ($n = 75$) tuned in both epochs. The RF indexes were highly significantly ($P < 0.001$) correlated. The equation of the linear regression line is also illustrated.

we plotted the ratio of hand-centered versus body-centered Euclidean distances (E_H/E_B, Fig. 4*B*). In both PLAN (Fig. 4*B*, top) and REACH (Fig. 4*B*, bottom), the distribution of the ratios was strongly biased toward ratio values <1, indicating a larger effect of modulations in body-centered coordinates.

We then examined how consistent were the RFs of single cells as the task progressed. Across the population of modulated cells, we found many cells ($n = 75$) that were tuned in both PLAN and REACH epochs. In these neurons, we used the Euclidean distance values to compute a unique RF index (RF, see Materials and Methods section). RF index provides a measure of the combined sensitivity to both frames and ranges from 0 (body-centered) to 1.414 (hand centered). When we compared the RF indexes of cells tuned in PLAN and REACH, we found that they were significantly correlated ($P < 0.001$, Fig. 4*C*). The RF index was higher for the population during the REACH epoch (Wilcoxon rank sum, $P < 0.0001$), thus indicating a strengthening of hand-centered coding. However, this effect was small as the mean RF increase in REACH was about 20%. The above analysis showed a high consistency of RFs as the task progressed.

In summary, the Euclidean distance analysis revealed that many V6A neurons encoded reaching targets in a mixed hand- and body-centered frame of reference and a comparable number of cells used exclusively a body-centered target representation. Only occasional units were found to encode reach goals in a hand-centered frame of reference.

Alternative Methods of Analysis of Reference Frames

In the literature on the frames of reference, inconsistencies between studies have been attributed to the different methods employed (Mullette-Gillman et al. 2009; McGuire and Sabes 2011; Bremner and Andersen 2012). In order to compensate for this, in addition to the correlation analysis and the

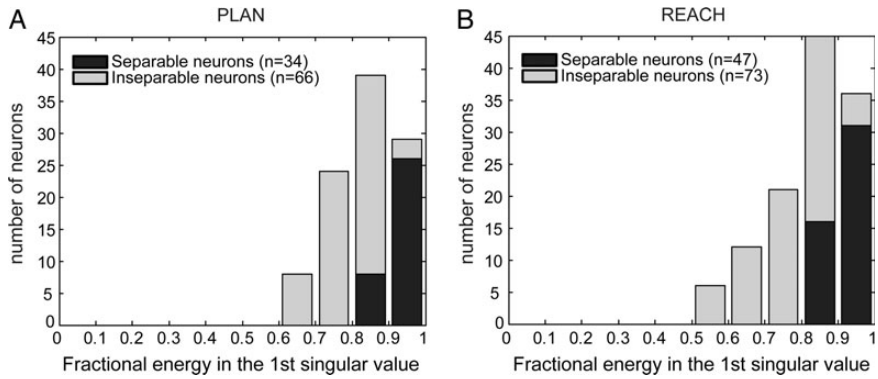

Figure 5. Separability analysis. Distrubutions of the fractional energy (FE) of the first singular value for all modulated neurons (separable and inseparable) in PLAN (*A*) and REACH (*B*). In both *A* and *B*, the distributions are shown for significantly ($P < 0.05$) separable ($n = 34$ in *A* and $n = 47$ in *B*) neurons and for the rest of the modulated neurons ($n = 66$ in *A* and $n = 73$ in *B*) that were found to be inseparable. The FE of the separable neurons was significantly higher than the inseparable ones (Kruskal–Wallis, $P < 0.05$). In both classes of neurons, the FE of the first singular value was high, thus suggesting an absence of target encoding relative to the hand (movement vector).

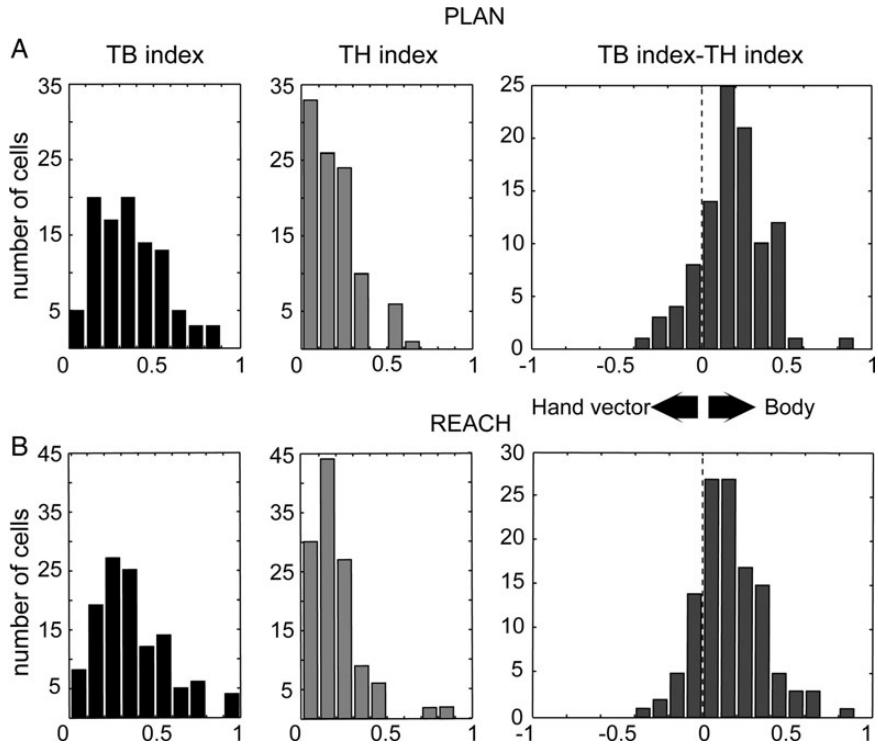

Figure 6. Strength of modulations by target and hand signals. The distribution of the modulation indexes T_B (left panels), T_H (middle panels) quantifying the strength of tuning of the activity in PLAN (*A*) and REACH (*B*) by changing the body and hand coordinates, respectively, of the target. The right panels in *A* and *B* illustrate the histogram of difference $T_B - T_H$. The vertical dashed line highlights that most values were positive.

comparison of the Euclidean distances, we performed 4 additional analyses adopted from recent studies of the RFs during reaching (Pesaran et al. 2006; Bhattacharyya et al. 2009; Blohm et al. 2009; Mullette-Gillman et al. 2009; Buneo and Andersen 2012).

In the first of these analyses, to define the RF of neural activity, we compared the mean firing rates across the conditions that were the same in one RF, but not in the other (Mullette-Gillman et al. 2005, 2009). To do this, we averaged the activity of each cell in all the pairs of conditions used for the correlation analysis (Fig. 3). The vast majority of the cells (80% in PLAN and 82% in REACH) showed a significant difference of average activity when target location relative to the body changed, but the movement vector remained the same. In contrast, only half of modulated cells (46% in PLAN and 57% in REACH) showed a significant change of firing rate when the target was reached with different movement vectors. The bootstrap analysis confirmed that in V6A the representation of targets in body-centered coordinates was more common than in hand-centered coordinates, but also showed that an important fraction of cells were influenced by the movement vector.

Another important analysis examined whether the starting hand position and the target location are encoded jointly or separately. To do this, we performed the singular value decomposition (SVD, see Materials and Methods section) analysis (Pesaran et al. 2006; Bhattacharyya et al. 2009). Using

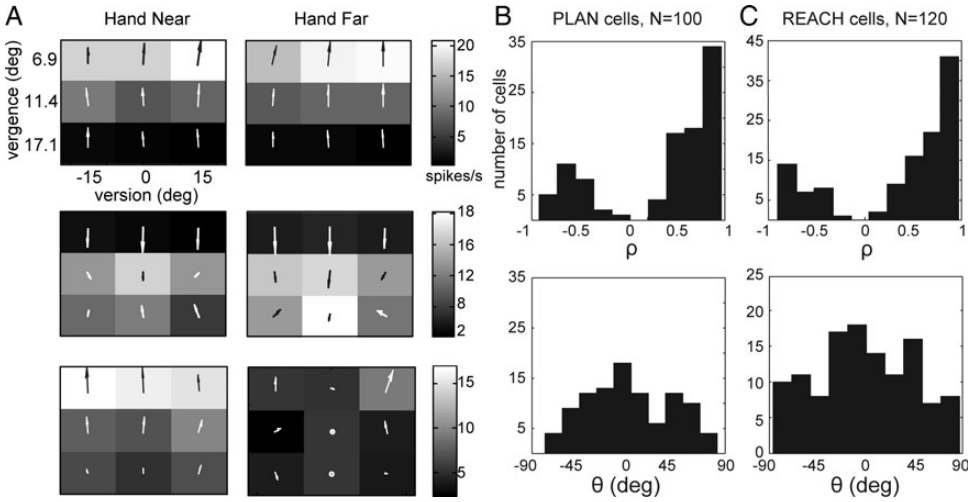

Figure 7. Vector correlation analysis. (*A*). Response fields and vector fields when reaching movements were made from a near (left plots) and a far (right plots) hand position. Top panel in *A* shows the response fields of the neuron of Figure 2*A* during REACH. The 2 fields were very similar, with the firing rate for the same target being almost identical. The field vectors converged on the peak of activity toward the far space (white and light gray squares). The vector correlation analysis for this cell yielded a correlation coefficient ρ equal to 0.98 and a difference in the angle (phase angle θ) between the vector fields that was −5°. In addition, the scaling factor β was 0.97. Middle panel in A: Response fields of the neuron of Figure 2*B* that was modulated only in REACH were well correlated with ρ, θ, and β equal to 0.87, 14°, and 1.02, respectively. Bottom panel in (*A*) Response fields of the neuron of Figure 2*C* for REACH. The coefficient ρ was −0.58, with the negative sign denoting that the responses were reflected along a given axis. The phase angle was −40°, much higher than in the previous neurons and β equal to 0.25. (*B,C*) Distribution of cofficient ρ (top panels) and phase angles θ (bottom panels) for the population of neurons modulated in PLAN (*B*) and REACH (*C*). It is evident that the majority of the V6A modulated neurons show high and positive coefficients ρ and low absolute values of phase angles θ.

this method, the neurons were classified into separable ones when their activity encoded target and hand position independently by a multiplicative coding mechanism and inseparable when this mechanism could not completely reconstruct the neural responses. We found that 34% and 39% of neurons modulated in PLAN and REACH, respectively, were classified as separable. To examine the degree of separability in the whole population of modulated neurons in both epochs, we computed the FE of the first singular value (Pena and Konishi 2001; Pesaran et al. 2006; Bhattacharyya et al. 2009). The distributions of this metric for the population are shown in Figure 5. The mean FE for the separable neurons in PLAN (Fig. 5*A*) was 0.92 ± 0.03, and in REACH (Fig. 5*B*) was 0.92 ± 0.04. For the inseperable neurons, the corresponding values were 0.79 ± 0.07 and 0.77 ± 0.1 for PLAN and REACH, respectively. The fact that also in the inseparable neurons the FE of the first singular value was still high (>0.55) suggests that rather than coding the movement vector (i.e., target relative to the hand), there is an intermediate encoding between target and hand position in the vast majority of these cells. In summary, the results of the SVD analysis indicate that V6A represents an intermediate stage of the transformations from body- to hand-centered coding, and thus are in line with the previous analyses.

To test between the 2 RFs, we also measured the strength of modulations in body- and hand-centered coordinates by calculating 2 indexes similar to those described by Bhattacharyya et al. (2009). The T_B index measured the modulation of cell activity when target position with respect to the body changed and movement vector remained stable (Fig. 6, left column). Index T_H quantified the modulation occurring when location of target changed relative to the hand, but remained the same with respect to the body (Fig. 6, middle column). For both indexes, a value of zero means that changing the target or hand position had no effect on the activity, while a value close to 1 indicates a maximum effect. An intermediate value of 0.33 means that the change of the target (T_B) and hand (T_H) position in space scales activity by a factor of 2 (doubling it or its reducing it to its half). On average, the 2 indexes were statistically different (Kolmogorov–Smirnov, $P < 0.05$) in both PLAN and REACH epoch. T_B index tended to be higher and more uniformly and widely distributed than T_H index. To compare the 2 indexes in individual neurons, we subtracted T_H from T_B index for each neuron and each epoch. A resulting value of zero indicates that the 2 modulations had equal strength in a given cell and epoch; positive values indicate that target location with respect to the body had more influence on cell activity than movement vector (target in hand coordinates), and negative values that changes in movement vector had a stronger effect than changes in target location with respect to the body. The majority of the V6A cells had positive values. The distribution of differences between T_B and T_H indexes was unimodal, shifted toward positive values (Fig. 6, right column). This finding argues against the case that there were 2 populations of V6A neurons, one encoding target position in body-centered and the other in hand-centered coordinates. In that case, the distribution of differences between T_B and T_H would have been bimodal and the neurons with positive and negative values would use body- and hand-centered frames of reference, respectively. Instead, our results show that most V6A cells encode both the body-centered target position and the hand movement vector, with the former having on average a stronger effect than the latter.

All the analyses presented so far do not take into account the overall 2D structure of the arm movement fields of single neurons, i.e. the fact that in our study targets were located at various depths and directions with precise spatial relationships. To examine this issue, we performed the vector correlation analysis that has been recently adopted as a tool to study the RFs (Buneo 2011; Buneo and Andersen 2012). This method provides a measure of correlation between 2 response

fields. In our case, the 2 response fields were the 2D (depth/vergence-direction/version) matrices of firing rates for movements that started from the near and the far button, respectively (Fig. 7). Our hypothesis was that if neurons encode targets in body-centered coordinates, the response fields should be strongly correlated because targets had the same location with respect to the body. In contrast, if neurons use hand-centered coordinates the correlation between the 2 response fields is expected to be much weaker. It should be noted that if the two matrices were identical (i.e., body centred RF) the vector correlation analysis would give a coefficient ρ and a phase angle θ of 1 and 0, respectively. The coefficient ρ is analogous to the Pearson linear correlation coefficient and the phase angle θ the amount of shift needed to align the 2 response fields (see Materials and Methods section). Figure 7*A* illustrates the mean activity during REACH for the three example neurons shown in Figure 2. The activity is represented as a response matrix where the discharges (gray scale) are plotted as a function of the vergence and version angle of each LED target. The arrows represent the vector of change in activity when moving from one target location to another. For each neuron, two matrices are depicted, for reaches that begun from the near (Fig. 7*A*, left plots) and from the far (Fig. 7*A*, right plots) initial hand position. For the first two neurons (Fig. 7*A*, top and middle panels), the vector correlation analysis yielded high values of ρ coefficients and small phase angles θ, thus verifying their consistent spatial tuning between the two different hand conditions. The effect of changing the initial hand position became evident in the neuron of Figure 2*C*, where the activity for most targets was altered significantly, especially in REACH epoch (Fig. 7*A*, bottom panel). Close inspection of the corresponding response fields shows that, on average, the activity for the near targets of the left panel was similar to the activity of far targets of the right panel (Fig. 7*A*, bottom panel). In summary, the analysis of the vector fields of the example neurons confirmed the results of the ANOVA and, in addition, quantified in more detail the changes in the 2D pattern of activity of single V6A neurons induced by manipulating the initial hand position.

We performed the same analysis for the whole population of the ANOVA modulated cells. As detailed previously, body-centered cells would show response matrices that are correlated with high and positive coefficients (ρ) and have a small phase angle (θ) difference between them. In contrast, cells with a strong effect of initial hand position would be more likely to have a medium to high value of the ρ coefficient with a negative sign, like the REACH activity of the example neuron of Figure 3*C*. The negative coefficient indicates that the 2 movement fields are reflected with respect to each other and this is due to the fact that in hand-centered coordinates the near targets from the near button are equivalent to the far targets of the far button (left). As shown in Figure 7*B*,*C*, the vast majority of neurons modulated in REACH and PLAN epochs had high and positive coefficients with phase angles that mostly ranged between ±30°. In addition, a small, but significant number of cells showed coefficients that were consistent with a strong influence of hand position. This finding is slightly different with respect to the results of the analysis of the Euclidean distance. It could be that in several of the cells defined as intermediate by the Euclidean distance, the vector correlation analysis makes more evident the hand position effect by considering the 2D structure of the movement field. Though, the vector correlation analysis was in line with the other methods and confirmed the prevalence of a body-centered representation in V6A.

Finally, we reconstructed the anatomical location of the recording sites and examined whether cells being more sensitive to a given RF were grouped together either across the cortical surface, or in depth. We did not find any anatomical segregation neither of the cellular types defined by the ANOVA analysis, nor for the categories of neurons classified with the Euclidean distance and the other analyses.

Discussion

In the present study, we examined whether, in area V6A, reach targets are encoded in hand or body-centered coordinates. We explored the 3D peripersonal space with targets located at different directions and depths. We found that most V6A cells encoded targets in a body-centered or in a mixed body- and hand-centered frame of reference during both preparation and execution of reaches in 3D space. We found very little evidence of pure hand-centered representations. Since the discrepancies between results of previous studies on frames of reference have been, at least in part, attributed to the different methods of analysis employed (Mullette-Gillman et al. 2009; Bremner and Andersen 2012), in order to test the validity of our results we additionally used here also the analytical approaches used in previous works (Fig.s 5–7) (Bhattacharyya et al. 2009; Mullette-Gillman et al. 2009; Buneo and Andersen 2012). All these different analyses confirmed our main findings, and in particular the poor evidence of pure hand-centered representation in V6A.

We did not find any significant difference in the relative representation of mixed and body-centered cells between planning and execution of reaching movements. In addition, the correlation of population activity in body- and hand-centered coordinates was similar in the 2 time epochs. These findings are consistent with previous reports on other PPC areas as PRR and LIP (Buneo et al. 2008; Mullette-Gillman et al. 2009; Chang and Snyder 2010), where the RFs of single neurons were stable during task evolution. All together these results suggest that the coordinate transformations during arm and eye movements do occur immediately after the target location input is received.

Given that area V6A is one of the earliest nodes of the parieto-frontal network that controls reaching movements (Galletti et al. 2003), and that more anterior areas in the PPC contain several cells where reach targets are represented in a hand frame of reference (see below; Chang and Snyder 2010; McGuire and Sabes 2011; Buneo and Andersen 2012), our findings support the view that the RF transformations from eye- to hand-centered representations occur gradually within this network, and in a caudo-rostral direction. In fact, area V6A has been previously shown to transform its retinocentric input mostly into mixed eye- and body-centered/spatiotopic coordinates, with smaller but still significant numbers of V6A neurons using either eye- or body-centered representations (Marzocchi et al. 2008). It should be mentioned that in the present study reaches were always performed toward foveated targets and the head was fixed relative to the body, so body-centered coordinates could not be distinguished from eye- and head-centered. Nonetheless, present results confirm that V6A is implicated in a number of coordinate transformations, including those leading to the construction of hand-centered target representations since many V6A neurons encode targets in mixed body- and hand-centered coordinates,

but only individual cells encode reaching targets only with reference to the hand. This means that the visuomotor transformations from eye- to hand-centered frame of reference do occur within V6A, but at this level of the PPC the intermediate representations are clearly the most typical outcome of these transformations, leaving to more anterior PPC areas the role of explicitly encoding targets relative to hand.

Also in many PPC areas other than V6A reaching targets are represented in mixed frames of reference (Mullette-Gillman et al. 2005, 2009; Chang and Snyder 2010; McGuire and Sabes 2011; Buneo and Andersen 2012). Whether this type of encoding simply reflects an intermediate step in the transition from one RF to another and therefore is an epiphenomenon of the RF transformation process, or whether it represents an alternative way of spatial encoding remains to be determined. Intermediate coding in the depth dimension has been reported also for the saccadic system in a neurophysiological study of the lateral intraparietal area (LIP) (Genovesio and Ferraina 2004). Most LIP neurons were found to combine, with variable weights, disparity, and vergence signals to represent saccadic targets in intermediate eye- and body/head-centered coordinates. Theoretical and modeling studies suggest that the intermediate representations could be beneficial to the computations that are necessary for the coordinates transformation in 3D space (Pouget and Snyder 2000; Blohm et al. 2009), and the present study, one of the first to address the RFs transformations in 3D space, is in accordance with this view. The strong presence of intermediate representations we observed in V6A is also one of the predictions of a recent modeling study addressing the computations of reach depth (Blohm 2012).

Hand-Related Signals in Other PPC Areas

The reported scarcity of hand-centered cells clearly distinguishes V6A from the nearby area PRR/MIP and from area 5, where a significant number of this type of cells was found (Chang and Snyder 2010; McGuire and Sabes 2011; Buneo and Andersen 2012). This functional distinction is in line with several human studies suggesting that the superior parieto-occipital cortex (SPOC), a putative human homologue of macaque V6A (Cavina-Pratesi et al. 2010), encodes the spatial location of movement goal, whereas more anterior areas along the medial bank of the intraparietal sulcus mainly process the movement vector (Fernandez-Ruiz et al. 2007; Filimon et al. 2009; Vesia et al. 2010; Davare et al. 2012). Alternatively, this dissimilarity between V6A and the other PPC areas in macaques could be due to differences in the experimental configuration between the aforementioned monkey studies and the present one. For example, differently from us, in previous studies center-out reaches were performed toward targets arranged on a single frontal plane and the starting hand locations were varied only in that plane. The center-out configuration allows a variety of reaches, both in upward and in downward directions to be executed, but the depth dimension is not tested. In our experiment, starting hand position was changed only in depth and only upward reaches against gravity were performed. However, we believe that these methodological differences cannot account for the fact that we did not find a significant number of hand-centered representations. In our experiment, hand position was manipulated so that reaches started from 2 quite distant positions in depth and this resulted in a comparable variety of reaching directions and amplitudes, including the movements having an opposite 3D vector (inward-outward). In addition, the changing of hand position in depth would be expected to exert a stronger influence on the reach-related activity, as several studies argue that the proprioceptive input from the hand is stronger in the depth dimension (Vindras et al. 1998; van Beers et al. 2004; Apker et al. 2010). Despite the fact that V6A receives substantial proprioceptive input (Breveglieri et al. 2002), very few hand-centered cells were found. Our experimental configuration is very similar to that used in a reaching in depth study in area 5 (Ferraina et al. 2009). In that work, the manipulation of starting hand position in depth had a strong effect on neural activity and many cells encoded the movement vector in hand-centered coordinates.

Our work reveals the presence in V6A of many neurons that encode reach target relative to the body, whereas a recent study in the reaching area PRR found no evidence of this type of coding (Buneo and Andersen 2012). In PPC, neurons using body/head-centered RFs have been reported in area LIP during saccades to visual and auditory targets (Mullette-Gillman et al. 2005, 2009). The fact that V6A encodes pure (body-centered) or partially transformed (mixed body- and hand-centered) spatiotopic representations, while PRR uses hand-centered and not body-centered representations suggests that the functional specializations among areas along the rostrocaudal axis of PPC are important for the parietofrontal network that controls arm movements. Both V6A and PRR project strongly to the dorsal premotor cortex (PMd) (Matelli et al. 1998; Gamberini et al. 2009), where overlapping populations of neurons that encode both the movement goal and the movement vector have been reported (Shen and Alexander 1997). Depending on the behavioral context PMd neurons could use one or another RF, as it has been shown in a recent functional imaging study (Bernier and Grafton 2010).

Funding

This work was supported by EU FP7-IST-217077-EYESHOTS, by Ministero dell'Università e della Ricerca (Italy), and by Fondazione del Monte di Bologna e Ravenna (Italy).

Notes

The authors thank Dr. A. Bosco and G. Dal Bo' for help in the recordings, A. Caroselli for help in data analysis and Drs L. Bremner and Y. Mokri for helpful discussions on reference frames. *Conflict of Interest:* None declared.

References

Apker GA, Darling TK, Buneo CA. 2010. Interacting noise sources shape patterns of arm movement variability in three-dimensional space. J Neurophysiol. 104:2654–2666.

Batista AP, Buneo CA, Snyder LH, Andersen RA. 1999. Reach plans in eye-centered coordinates. Science. 285:257–260.

Batista AP, Santhanam G, Yu BM, Ryu SI, Afshar A, Shenoy KV. 2007. Reference frames for reach planning in macaque dorsal premotor cortex. J Neurophysiol. 98:966–983.

Bernier PM, Grafton ST. 2010. Human posterior parietal cortex flexibly determines reference frames for reaching based on sensory context. Neuron. 68:776–788.

Bhattacharyya R, Musallam S, Andersen RA. 2009. Parietal reach region encodes reach depth using retinal disparity and vergence angle signals. J Neurophysiol. 102:805–816.

Blohm G. 2012. Simulating the Cortical 3D visuomotor transformation of reach depth. PLoS One. 7:e41241.

Blohm G, Keith GP, Crawford JD. 2009. Decoding the cortical transformations for visually guided reaching in 3D space. Cereb Cortex. 19:1372–1393.
Bremner L, Andersen R. 2012. Coding of the reach vector in parietal area 5D. Neuron. 75:342–351.
Breveglieri R, Kutz DF, Fattori P, Gamberini M, Galletti C. 2002. Somatosensory cells in the parieto-occipital area V6A of the macaque. Neuroreport. 13:2113–2116.
Buneo C, Batista A, Jarvis M, Andersen R. 2008. Time-invariant reference frames for parietal reach activity. Exp Brain Res. 188:77–89.
Buneo CA. 2011. Analyzing neural responses with vector fields. J Neurosci Methods. 197:109–117.
Buneo CA, Andersen RA. 2012. Integration of target and hand position signals in the posterior parietal cortex: effects of workspace and hand vision. J Neurophysiol. 108:187–199.
Buneo CA, Jarvis MR, Batista AP, Andersen RA. 2002. Direct visuomotor transformations for reaching. Nature. 416:632–636.
Cavina-Pratesi C, Monaco S, Fattori P, Galletti C, McAdam TD, Quinlan DJ, Goodale MA, Culham JC. 2010. Functional magnetic resonance imaging reveals the neural substrates of arm transport and grip formation in reach-to-grasp actions in humans. J Neurosci. 30: 10306–10323.
Chang SW, Papadimitriou C, Snyder LH. 2009. Using a compound gain field to compute a reach plan. Neuron. 64:744–755.
Chang SWC, Dickinson AR, Snyder LH. 2008. Limb-specific representation for reaching in the posterior parietal cortex. J Neurosci. 28:6128–6140.
Chang SWC, Snyder LH. 2010. Idiosyncratic and systematic aspects of spatial representations in the macaque parietal cortex. Proc Natl Acad Sci. 107:7951–7956.
Davare M, Zenon A, Pourtois G, Desmurget M, Olivier E. 2012. Role of the medial part of the intraparietal sulcus in implementing movement direction. Cereb Cortex. 22:1382–1394.
Fattori P, Gamberini M, Kutz DF, Galletti C. 2001. "Arm-reaching" neurons in the parietal area V6A of the macaque monkey. Eur J Neurosci. 13:2309–2313.
Fattori P, Kutz DF, Breveglieri R, Marzocchi N, Galletti C. 2005. Spatial tuning of reaching activity in the medial parieto-occipital cortex (area V6A) of macaque monkey. Eur J Neurosci. 22:956–972.
Fernandez-Ruiz J, Goltz HC, DeSouza JF, Vilis T, Crawford JD. 2007. Human parietal "reach region" primarily encodes intrinsic visual direction, not extrinsic movement direction, in a visual motor dissociation task. Cereb Cortex. 17:2283–2292.
Ferraina S, Brunamonti E, Giusti MA, Costa S, Genovesio A, Caminiti R. 2009. Reaching in depth: hand position dominates over binocular eye position in the rostral superior parietal lobule. J Neurosci. 29:11461–11470.
Filimon F, Nelson JD, Huang RS, Sereno MI. 2009. Multiple parietal reach regions in humans: cortical representations for visual and proprioceptive feedback during on-line reaching. J Neurosci. 29:2961–2971.
Flanders M, Helms Tillery SI, Soechting JF. 1992. Early stages in a sensorinotor transformation. Behav Brain Sci. 15:309–362.
Galletti C, Battaglini PP, Fattori P. 1995. Eye position influence on the parieto-occipital area PO (V6) of the macaque monkey. Eur J Neurosci. 7:2486–2501.
Galletti C, Fattori P, Battaglini PP, Shipp S, Zeki S. 1996. Functional demarcation of a border between areas V6 and V6A in the superior parietal gyrus of the macaque monkey. Eur J Neurosci. 8:30–52.
Galletti C, Fattori P, Kutz DF, Gamberini M. 1999. Brain location and visual topography of cortical area V6A in the macaque monkey. Eur J Neurosci. 11:575–582.
Galletti C, Kutz D, Gamberini M, Breveglieri R, Fattori P. 2003. Role of the medial parieto-occipital cortex in the control of reaching and grasping movements. Exp Brain Res. 153:158–170.
Gamberini M, Galletti C, Bosco A, Breveglieri R, Fattori P. 2011. Is the medial posterior parietal area V6A a single functional area? J Neurosci. 31:5145–5157.
Gamberini M, Passarelli L, Fattori P, Zucchelli M, Bakola S, Luppino G, Galletti C. 2009. Cortical connections of the visuomotor parietooccipital area V6Ad of the macaque monkey. J Comp Neurol. 513: 622–642.
Genovesio A, Ferraina S. 2004. Integration of retinal disparity and fixation-distance related signals toward an egocentric coding of distance in the posterior parietal cortex of primates. J Neurophysiol. 91:2670–2684.
Hanson B, Klink K, Matsuura K, Robeson SM, Willmott CJ. 1992. Vector correlation: review, exposition, and geographic application. Ann Assoc Am Geog. 82:103–116.
Kutz DF, Fattori P, Gamberini M, Breveglieri R, Galletti C. 2003. Early- and late-responding cells to saccadic eye movements in the cortical area V6A of macaque monkey. Exp Brain Res. 149:83–95.
Kutz DF, Marzocchi N, Fattori P, Cavalcanti S, Galletti C. 2005. Real-time supervisor system based on trinary logic to control experiments with behaving animals and humans. J Neurophysiol. 93:3674–3686.
Lacquaniti F, Guigon E, Bianchi L, Ferraina S, Caminiti R. 1995. Representing spatial information for limb movement: role of area 5 in the monkey. Cereb Cortex. 5:391–409.
Luppino G, Ben Hamed S, Gamberini M, Matelli M, Galletti C. 2005. Occipital (V6) and parietal (V6A) areas in the anterior wall of the parieto-occipital sulcus of the macaque: a cytoarchitectonic study. Eur J Neurosci. 21:3056–3076.
Marzocchi N, Breveglieri R, Galletti C, Fattori P. 2008. Reaching activity in parietal area V6A of macaque: eye influence on arm activity or retinocentric coding of reaching movements? Eur J Neurosci. 27: 775–789.
Matelli M, Govoni P, Galletti C, Kutz DF, Luppino G. 1998. Superior area 6 afferents from the superior parietal lobule in the macaque monkey. J Comp Neurol. 402:327–352.
McGuire LM, Sabes PN. 2011. Heterogeneous representations in the superior parietal lobule are common across reaches to visual and proprioceptive targets. J Neurosci. 31:6661–6673.
Mullette-Gillman ODA, Cohen YE, Groh JM. 2005. Eye-centered, head-centered, and complex coding of visual and auditory targets in the intraparietal sulcus. J Neurophysiol. 94:2331–2352.
Mullette-Gillman ODA, Cohen YE, Groh JM. 2009. Motor-related signals in the intraparietal cortex encode locations in a hybrid, rather than eye-centered reference frame. Cereb Cortex. 19:1761–1775.
Pena JL, Konishi M. 2001. Auditory spatial receptive fields created by multiplication. Science. 292:249–252.
Pesaran B, Nelson MJ, Andersen RA. 2006. Dorsal premotor neurons encode the relative position of the hand, eye, and goal during reach planning. Neuron. 51:125–134.
Pouget A, Snyder LH. 2000. Computational approaches to sensorimotor transformations. Nat Neurosci. 3(Suppl):1192–1198.
Shen L, Alexander GE. 1997. Preferential representation of instructed target location versus limb trajectory in dorsal premotor area. J Neurophysiol. 77:1195–1212.
van Beers RJ, Haggard P, Wolpert DM. 2004. The role of execution noise in movement variability. J Neurophysiol. 91: 1050–1063.
Vesia M, Prime SL, Yan X, Sergio LE, Crawford JD. 2010. Specificity of human parietal saccade and reach regions during transcranial magnetic stimulation. J Neurosci. 30:13053–13065.
Vindras P, Desmurget M, Prablanc C, Viviani P. 1998. Pointing errors reflect biases in the perception of the initial hand position. J Neurophysiol. 79:3290–3294.
Zar J. 1999. Biostatistical Analysis. Upper Saddle River, New Jersey: Prentice-Hall.